Early initiation of a factor Xa inhibitor can attenuate tissue repair and neurorestoration after middle cerebral artery occlusion

古森, 元浩

https://doi.org/10.15017/4059952

出版情報：Kyushu University, 2019, 博士（医学）, 課程博士
バージョン：

Brain Research 1718 (2019) 201–211

Contents lists available at ScienceDirect

Brain Research

journal homepage: www.elsevier.com/locate/brainres

Research report

Early initiation of a factor Xa inhibitor can attenuate tissue repair and neurorestoration after middle cerebral artery occlusion

Motohiro Komori, Tetsuro Ago*, Yoshinobu Wakisaka, Kuniyuki Nakamura, Masaki Tachibana, Yoji Yoshikawa, Tomoya Shibahara, Kei Yamanaka, Junya Kuroda, Takanari Kitazono

Department of Medicine and Clinical Science, Graduate School of Medical Sciences, Kyushu University, 3-1-1 Maidashi, Higashi-ku, Fukuoka 812-8582, Japan

HIGHLIGHTS

- Factor Xa inhibitor may attenuate peri-infarct astrogliosis and neurorestoration after pMCAO.
- Factor Xa inhibitor may attenuate leptomeningeal anastomosis development after pMCAO.
- Factor Xa inhibitor may attenuate angiogenesis and fibrotic changes in ischemic areas.
- Factor Xa inhibitor may enhance inflammatory responses by attenuating tissue repair.
- The negative effects of factor Xa inhibitor are not found in ischemia/reperfusion stroke model.

ARTICLE INFO

Keywords:
Acute ischemic stroke
Angiogenesis
Arteriogenesis
Direct oral anticoagulant
Neurorestoration

ABSTRACT

The timing of anti-coagulation therapy initiation after acute cardioembolic stroke remains controversial. We investigated the effects of post-stroke administration of a factor Xa inhibitor in mice, focusing on tissue repair and functional restoration outcomes. We initiated administration of rivaroxaban, a Xa inhibitor, immediately after permanent distal middle cerebral artery occlusion (pMCAO) in CB-17 mice harboring few leptomeningeal anastomoses at baseline. Rivaroxaban initiated immediately after pMCAO hindered the recovery of blood flow in ischemic areas by inhibiting leptomeningeal anastomosis development, and led to impaired restoration of neurologic functions with less extensive peri-infarct astrogliosis. Within infarct areas, angiogenesis and fibrotic responses were attenuated in rivaroxaban-fed mice. Furthermore, inflammatory responses, including the accumulation of neutrophils and monocytes/macrophages, local secretion of pro-inflammatory cytokines, and breakdown of the blood–brain barrier, were enhanced in infarct areas in mice treated immediately with rivaroxaban following pMCAO. The detrimental effects were not found when rivaroxaban was initiated after transient MCAO or on day 7 after pMCAO. Collectively, early post-stroke initiation of a factor Xa inhibitor may suppress leptomeningeal anastomosis development and blood flow recovery in ischemic areas, thereby resulting in attenuated tissue repair and functional restoration unless occluded large arteries are successfully recanalized.

1. Introduction

Stroke is a leading cause of death and disability worldwide. Cardioembolic stroke is the most severe stroke subtype and often occurs in elderly subjects with atrial fibrillation, and can render elderly subjects bedridden and requiring care. Thus, when physicians identify atrial fibrillation, particularly in elderly subjects, they should initiate anti-coagulation therapy for the primary prevention of cardioembolic stroke (Gage et al., 2001). In addition, when physicians encounter patients with acute cardioembolic stroke with atrial fibrillation, they need to initiate anti-coagulation therapy at an appropriate time to prevent the recurrence of cardioembolism and to avoid massive hemorrhagic transformation that may worsen neurologic symptoms (Berger et al., 2001). In clinical practice, the timing of anti-coagulation therapy

Abbreviations: ACA, anterior cerebral artery; BBB, blood–brain barrier; CCR, C-C chemokine receptor; CXCR, C-X-C chemokine receptor; DOAC, direct oral anticoagulant; EBST, elevated body swing test; GFAP, glial fibrillary acidic protein; MAP-2, microtubule-associated protein 2; PAR, protease-activated receptor; PCA, posterior cerebral artery; PDGFRβ, platelet derived growth factor receptor β; pMCAO, permanent middle cerebral artery occlusion; PT-INR, prothrombin time-international normalized ratio; rt-PA, recombinant tissue-plasminogen activator; tMCAO, transient middle cerebral artery occlusion

* Corresponding author.
E-mail address: agou@intmed2.med.kyushu-u.ac.jp (T. Ago).

https://doi.org/10.1016/j.brainres.2019.05.020
Received 19 February 2019; Received in revised form 14 May 2019; Accepted 16 May 2019
Available online 16 May 2019
0006-8993/

initiation after acute cardioembolic stroke remains controversial. AHA/ASA guidelines do not recommend the use of anti-coagulants earlier than 14 days after the onset of cardioembolic stroke (Kernan et al., 2014), while the European Heart Rhythm Association Practical Guide proposes a "1-3-6-12 rule" for the timing of anti-coagulation therapy initiation, depending on stroke size and neurologic severity (Heidbuchel et al., 2013). Recently, direct oral anti-coagulants (DOAC) have been used for the prevention of cardioembolic stroke. Because DOAC are thought to avoid massive hemorrhagic complications compared with warfarin, it is hypothesized that DOAC could be used earlier after cardioembolic stroke (Gioia et al., 2016; Ploen et al., 2014). Furthermore, factor Xa and thrombin may function as pro-inflammatory factors through the activation of protease-activated receptors (PARs) (Vergnolle et al., 2001). Post-stroke inflammation is an important factor in worsening functional outcomes after ischemic stroke (Shichita et al., 2012), and high concentrations of thrombin may directly kill neurons and astrocytes (Striggow et al., 2000; Vergnolle et al., 2001). Thus, it is expected that inhibitors of factor Xa or thrombin may attenuate post-stroke inflammation and neuronal death without causing massive hemorrhagic transformation after acute cardioembolic stroke. On the other hand, because factor Xa and thrombin can also promote angiogenesis and fibrotic responses (Mercer and Chambers, 2013; Uusitalo-Jarvinen et al., 2007), it is possible that the inhibitors rather hinder tissue repair leading to neurorestoration. Recently, Ploen et al. demonstrated that pre-treatment with rivaroxaban did not have any detrimental effects, including hemorrhage or the breakdown of the blood–brain barrier (BBB), in a 2-hour transient middle cerebral artery occlusion (tMCAO) followed by thrombolytic therapy with recombinant tissue-plasminogen activator (rt-PA) in mice (Ploen et al., 2014). However, in clinical settings, it is unusual that anti-coagulation therapy can be initiated just before or immediately after successful thrombolysis with such a short period of ischemic time.

In the present study, we tested whether anti-coagulation therapy using a factor Xa inhibitor could be beneficially and safely initiated after a permanent MCAO (pMCAO) stroke model, focusing particularly on the recovery of cerebral blood flow, neurologic restoration, and tissue repair including fibrotic formation, peri-infarct astrogliosis, and inflammation. In the present study, to precisely evaluate the post-stroke development of leptomeningeal anastomoses (=arteriogenesis), we used CB-17 mice. These are a derivative of BALB mice that, when healthy, have few leptomeningeal anastomoses between the MCA and anterior cerebral artery (ACA) or posterior cerebral artery (PCA) (Tachibana et al., 2017; Zhang et al., 2010). Thus, it should be noted that the development of leptomeningeal anastomoses is absolutely needed for the recovery of blood flow in ischemic areas after pMCAO. In addition, due to few leptomeningeal anastomoses at baseline, infarct volume produced by tMCAO with more than 60 min ischemia is almost similar as that by pMCAO in CB-17 mice (Tachibana et al., 2017).

2. Results

2.1. Initiation of rivaroxaban treatment immediately after pMCAO attenuates functional restoration with reduced astrogliosis in peri-infarct areas

We first examined the effects of initiating rivaroxaban treatment immediately after pMCAO on infarct volume in CB-17 mice. Immunohistochemistry results demonstrated that microtubule-associated protein 2 (MAP-2)-negative areas (Fig. 1A) and infarct volume (Fig. 1B) were not significantly different between vehicle-fed (control) and rivaroxaban-fed mice. The MAP-2-negative areas gradually reduced from day 4 after pMCAO in both groups. However, from day 5 after pMCAO, neurologic function as assessed by elevated body swing test (EBST) recovered better in control mice than in rivaroxaban-fed mice (Fig. 1C). Additionally, immunohistochemical results demonstrated that the extent of glial fibrillary acidic protein (GFAP)-positive astrogliosis in peri-infarct areas was significantly attenuated in rivaroxaban-fed mice (Fig. 1D and E). GFAP expression levels in the ischemic hemisphere were also lower in rivaroxaban-fed mice compared with controls, as demonstrated by immunoblot analysis (Fig. 1F).

2.2. Immediate initiation of rivaroxaban treatment after pMCAO attenuates leptomeningeal anastomosis development

To investigate why rivaroxaban treatment attenuated peri-infarct astrogliosis and functional restoration, we examined blood flow recovery in ischemic areas after pMCAO. Because it is known that CB-17 mice have few leptomeningeal anastomoses at baseline under healthy conditions, in these mice the effective anastomoses between the MCA and ACA or PCA have to develop to recover blood flow in ischemic areas after pMCAO. In control mice, leptomeningeal anastomoses gradually developed over 4 days after pMCAO (Fig. 2A). However, the formation of leptomeningeal anastomoses on day 7 after pMCAO was markedly reduced in rivaroxaban-fed mice compared with controls (Fig. 2A). Consistently, the cerebral blood flow in ischemic areas was reduced on day 7 after pMCAO in rivaroxaban-fed mice (Fig. 2B). Although the average diameter of newly developed collateral arteries was not significantly different between control and rivaroxaban-fed mice on day 7 after pMCAO, the number of detectable collaterals was significantly lower in rivaroxaban-fed mice (Fig. 2C). Consistent with the extent of leptomeningeal anastomosis development, we discovered that mature angiogenesis within infarct areas, as assessed by immunostaining of platelet-derived growth factor receptor β (PDGFRβ)-expressing mural cells (Bodnar et al., 2013), was fewer in rivaroxaban-fed mice on day 7 after pMCAO (Fig. 2D).

2.3. Rivaroxaban may attenuate angiogenesis and fibrotic changes in ischemic areas after pMCAO, possibly through PAR-1 and PAR-2

We next examined the mechanisms of rivaroxaban's attenuation of leptomeningeal anastomosis development and angiogenesis within infarct areas after pMCAO. Factor Xa and thrombin are known to activate PARs, mainly PAR-1 and PAR-2, and may play important roles in arteriogenesis/angiogenesis (Battinelli et al., 2014; Katsanos et al., 2009). Immunohistochemical results demonstrated that both PAR-1 and PAR-2 were highly expressed within ischemic areas, but there were much fewer PAR-1- and PAR-2-positive cells in peri-infarct areas that contained astrocytes and neurons (Fig. 3A). In addition, both PAR-1 and PAR-2 were expressed in PDGFRβ-positive vascular cells (=pericytes, arrowheads) near superficial cortical areas (Fig. 3B) and in small vessels within the ischemic core (Fig. 3C).

We also demonstrated that cultured brain pericytes expressed both PAR-1 and PAR-2 (Fig. 3D). Treatment with factor Xa increased the cell number, while reducing cell death, in cultured pericytes (Fig. 3E and F). Additional treatment with the PAR-1 inhibitor vorapaxar and/or the PAR-2 inhibitor GB83 as well as rivaroxaban significantly reduced cell numbers, while increasing cell death (Fig. 3E and F). These results suggested that factor Xa promotes the survival/growth of PDGFRβ-positive pericytes through PAR-1/PAR-2 within infarct areas.

We and others previously demonstrated that PDGFRβ-positive pericytes proliferate within infarct areas and promote tissue repair in a subacute phase (Makihara et al., 2015; Tachibana et al., 2017). Immunostaining of PDGFRβ within infarct areas was attenuated on day 10 after pMCAO in rivaroxaban-fed mice (Fig. 3G), and immunoblot analysis using brain homogenates prepared from the ischemic hemisphere confirmed that PDGFRβ expression was lower in rivaroxaban-fed mice than in control mice (Fig. 3H).

2.4. Initiation of rivaroxaban treatment immediately after pMCAO enhances inflammatory responses within ischemic areas

We further examined the effects of immediate rivaroxaban

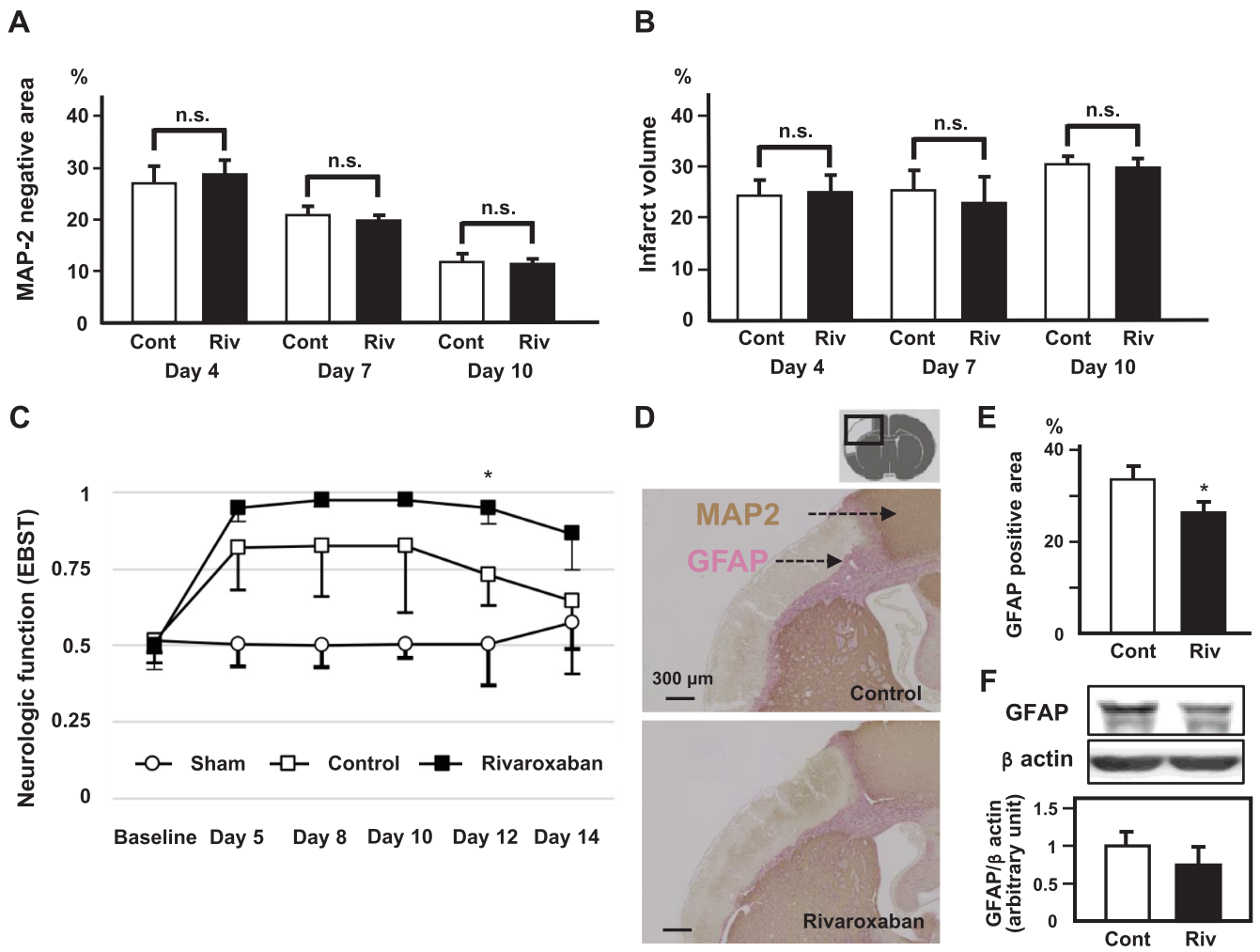

Fig. 1. Effects of rivaroxaban initiation immediately after pMCAO. Microtubule-associated protein 2 (MAP-2) negative areas (A) and infarct volume (B) on days 4, 7, and 10 after permanent middle cerebral artery occlusion (pMCAO) in control (Cont) and rivaroxaban-fed (Riv) mice (n = 4; ns, not significant). (C) Neurologic function, assessed by elevated body swing test (EBST) on days 5, 8, 10, 12, and 14 after pMCAO, is shown in sham (non-pMCAO; open circle), control (open square), and rivaroxaban-fed (closed square) mice. Values are means ± S.D. (n = 5; *p < 0.05). (D) Representative images of immunohistochemical double labeling for MAP-2 (brown) and glial fibrillary acidic protein (GFAP) (purple) on day 10 after pMCAO. (E) Quantification of the GFAP-positive area in control and rivaroxaban-fed mice (n = 4; *p < 0.05). (F) Immunoblot analysis of GFAP and β-actin in control and rivaroxaban-fed mice using homogenates prepared from the ischemic hemisphere on day 10 after pMCAO. Values are means ± S.D (n = 5).

treatment on inflammatory responses within infarct areas after pMCAO. Immunohistochemical staining demonstrated that there were greater numbers of Ly6G-positive neutrophil in ischemic areas on day 4 after pMCAO in rivaroxaban-fed mice than control mice (Fig. 4A). Additionally, expression levels of the neutrophil markers CXCR1 and CXCR2 were significantly higher in rivaroxaban-fed mice, as shown by quantitative PCR using RNA prepared from the ischemic hemisphere (Fig. 4B). In rivaroxaban-fed mice, there was also greater accumulation of F4/80-positive monocytes/macrophages in peri-infarct areas (Fig. 4C), and using quantitative PCR there was significantly higher expression of CCR2, a marker of monocytes/macrophages, compared with controls (Fig. 4D). Moreover, using quantitative PCR we demonstrated that, among the major pro-inflammatory cytokines TNFα, IL-1β, and IL-6, expression of TNFα in the ischemic hemisphere was significantly higher in rivaroxaban-fed mice on day 7 after pMCAO (Fig. 4E). Consistent with the enhanced inflammatory responses in rivaroxaban-fed mice, the breakdown of the BBB, as assessed by the leakage of Evans blue dye (Fig. 4F and G), and the hemorrhagic score (Ploen et al., 2014) (Fig. 4H) were significantly greater on day 4 after pMCAO compared with controls, although massive hemorrhagic transformation was not found even in rivaroxaban-fed mice.

2.5. Immediate rivaroxaban treatment after tMCAO and delayed rivaroxaban treatment after pMCAO do not affect functional restoration or pathological changes

Finally, we tested the effects of rivaroxaban treatment initiated immediately after tMCAO (90 min ischemia and reperfusion) on functional restoration, MAP2-negative infarct areas, infarct volume and peri-infarct astrogliosis. In contrast to the pMCAO model, rivaroxaban treatment initiated immediately after tMCAO neither deteriorated functional restoration (Fig. 5A) nor affected the MAP2-negative area, infarct volume and peri-infarct astrogliosis (Fig. 5B). We also tested the effects of delayed rivaroxaban treatment, initiated on day 7 after pMCAO. The delayed administration of rivaroxaban did not affect functional restoration (Fig. 5C) or the pathohistological changes (Fig. 5D).

3. Discussion

In the present study, we demonstrated that initiating treatment with the factor Xa inhibitor rivaroxaban immediately after pMCAO hindered the recovery of blood flow in ischemic areas, at least partly through the inhibition of leptomeningeal anastomosis development, and impaired

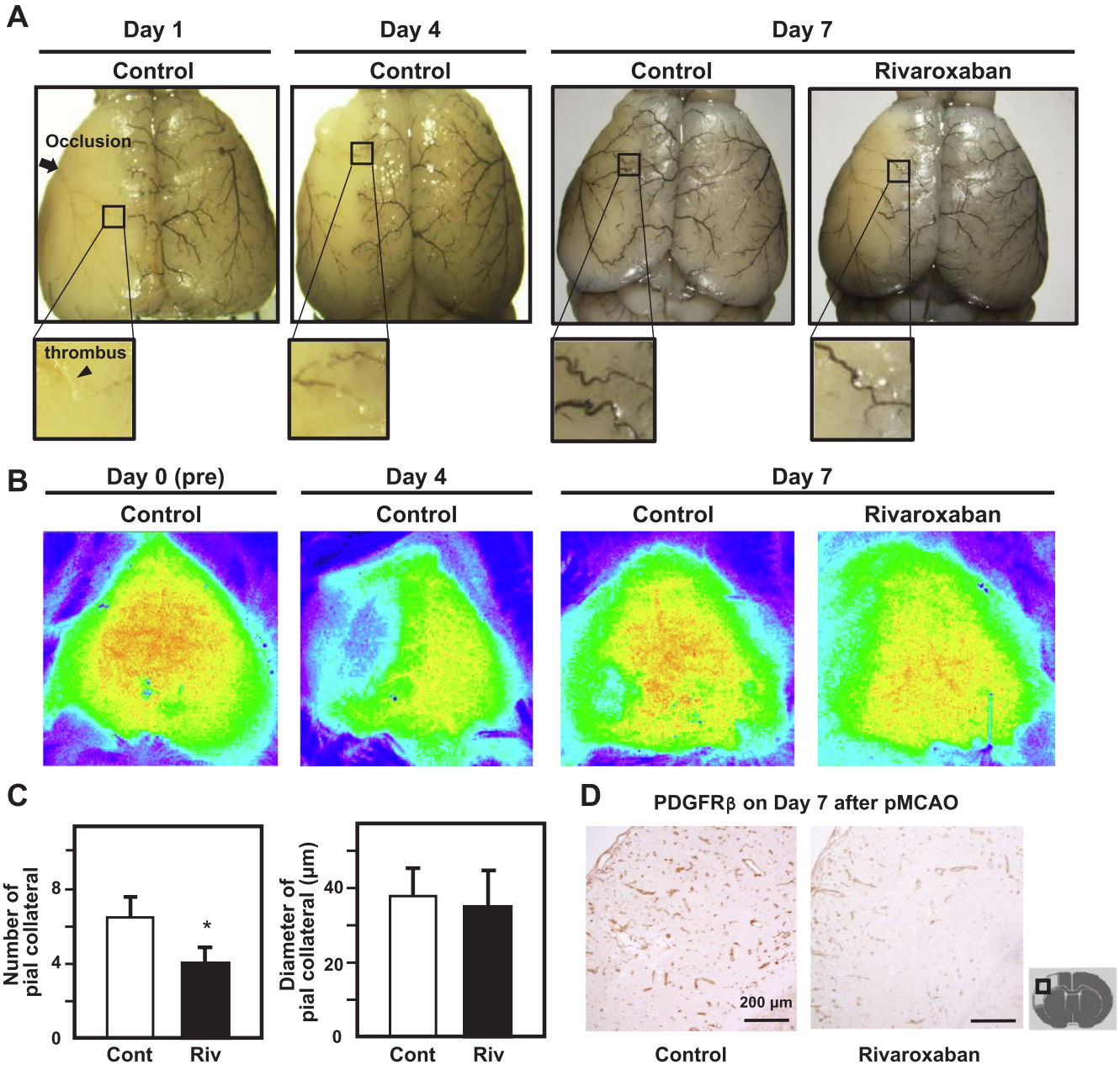

Fig. 2. Effects of rivaroxaban initiation immediately after pMCAO on leptomeningeal anastomosis development and mature angiogenesis within infarct area. (A) Leptomeningeal angioarchitecture was assessed by latex perfusion on days 1, 4, and 7 after pMCAO in control mice, and on day 7 after pMCAO in rivaroxaban-fed mice ($n = 4$). The arrow (in the left panel) signals the occlusion site. (B) Representative images of cerebral blood flow assessed by a 2D flowmeter on days 0 (pre-pMCAO), 4, and 7 after pMCAO ($n = 4$). (C) Number (left) and average diameter (right) of leptomeningeal anastomoses between the MCA and ACA or PCA ($n = 4$; $^*p < 0.05$). (D) Representative images of mature angiogenesis, assessed by immunohistochemistry of anti-platelet-derived growth factor receptor β (PDGFRβ), in the ischemic core in control and rivaroxaban-fed mice on day 7 after pMCAO ($n = 4$).

the restoration of neurologic functions. Both peri-infarct astrogliosis and intra-infarct fibrotic responses were significantly attenuated in rivaroxaban-fed mice. PAR-1 and PAR-2, targets of factor Xa, were expressed in PDGFRβ-positive pericytes within ischemic areas. PAR-1 or PAR-2 inhibitors as well as rivaroxaban significantly decreased factor Xa-mediated pericyte survival/growth. In rivaroxaban-fed mice, impaired repair processes in ischemic areas were accompanied by enhanced inflammatory responses and BBB breakdown. The detrimental effects of rivaroxaban on neurologic functions and histological changes were not observed when the treatment was initiated on day 7 after pMCAO or immediately after tMCAO.

3.1. Factor Xa inhibition attenuates leptomeningeal anastomosis development, thereby reducing blood flow recovery in ischemic areas after pMCAO

In the present study, we used CB-17 mice, which are a derivative of BALB mice, and which have the fewest number of leptomeningeal anastomoses under healthy conditions among mice commonly used for experiments (Tachibana et al., 2017; Zhang et al., 2010). Thus, new development of effective leptomeningeal anastomoses from the ACA or PCA after pMCAO are absolutely needed to recover blood flow in ischemic areas. Fig. 2 clearly demonstrates that CB-17 mice are able to develop leptomeningeal anastomoses and recover blood flow within ischemic areas over 5–7 days after pMCAO (Zhang et al., 2010).

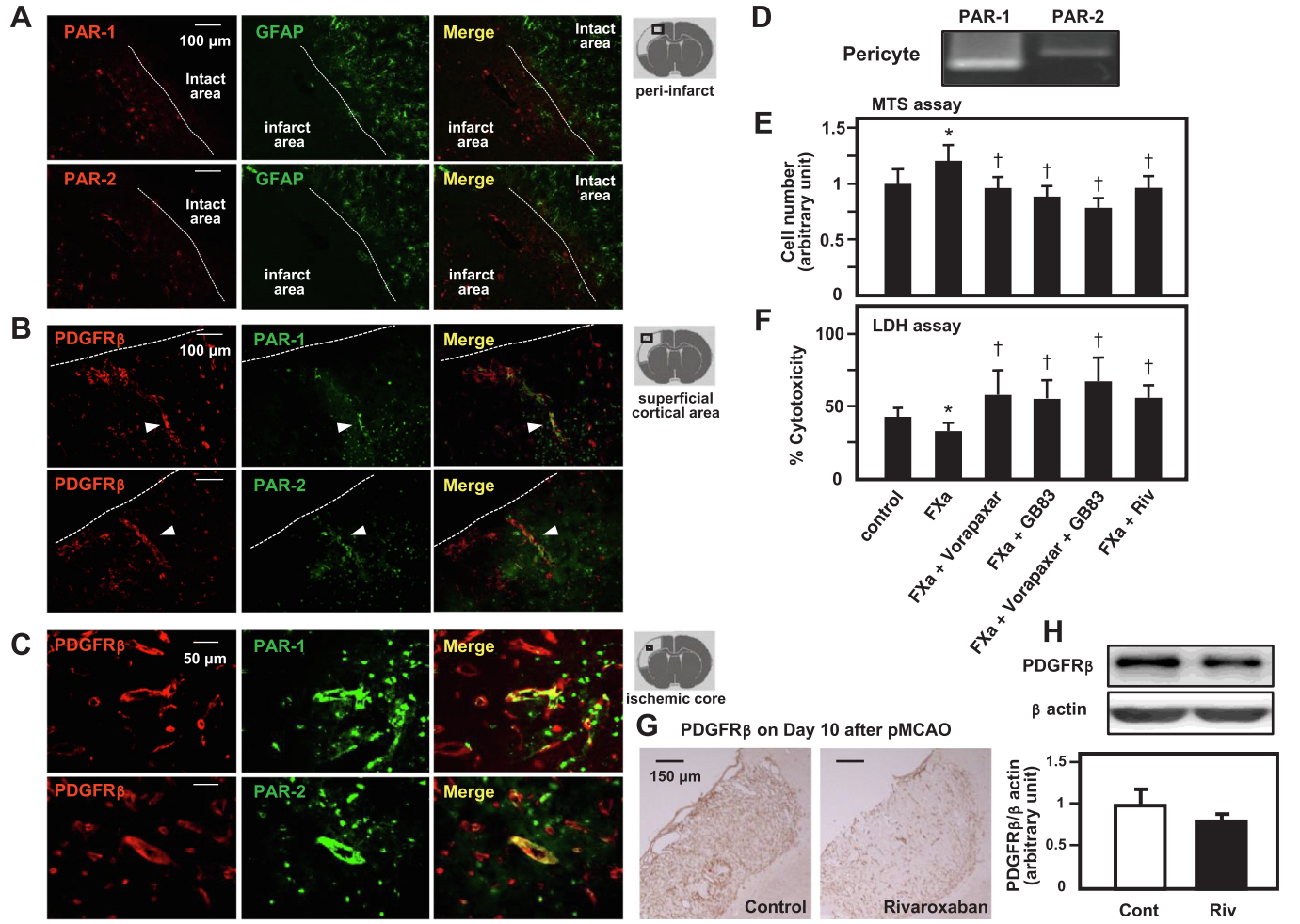

Fig. 3. Factor Xa-mediated angiogenesis and fibrotic changes within ischemic areas through PAR-1 and PAR-2. (A) Representative immunofluorescence double labelling for protease-activated receptor (PAR)-1 (**top**) or PAR-2 (**bottom**) (red) and GFAP (green) in peri-infarct areas on day 7 after pMCAO. Representative immunofluorescence double labelling for PAR-1 (**top**) or PAR-2 (**bottom**) (green) and PDGFRβ (red) in superficial cortical areas (B) and within ischemic cores (C) on day 7 after pMCAO. (D) mRNA expression of PAR-1 and PAR-2 in cultured human brain pericytes. Effects of the PAR-1 inhibitor vorapaxar (5 μmol/L), the PAR-2 inhibitor GB83 (10 μmol/L), and rivaroxaban (10 μmol/L) on factor Xa (FXa)-mediated growth assessed by MTT assay (E) and survival by LDH assay (F) in cultured pericytes. Values are means ± S.D. ($n = 8$; $^{*}p < 0.05$ vs. control and $^{\dagger}p < 0.05$ vs. FXa). (G) Representative immunohistochemistry for PDGFRβ in the ischemic core on day 10 after pMCAO ($n = 4$). (h) Immunoblot analysis of PDGFRβ in the ischemic hemisphere on day 10 after pMCAO ($n = 5$).

However, the initiation of rivaroxaban treatment immediately after pMCAO reduced arteriogenesis and blood flow recovery in ischemic areas. We speculate that the attenuated arteriogenesis and blood flow recovery in ischemic areas was the primary cause of decreased neurorestoration after pMCAO in rivaroxaban-fed mice because it is known that the recovery of blood flow in ischemic areas is an indispensable factor leading to post-stroke neurorestoration in peri-infarct areas (Chen et al., 2014; Renner et al., 2003).

3.2. Factor Xa may play an important role in survival/growth in pericytes within ischemic areas, particularly after pMCAO

Factor Xa and its downstream coagulation factor thrombin can act directly on PARs, mainly PAR-1 and PAR-2 (Ossovskaya and Bunnett, 2004). It is believed that PAR-1 and PAR-2 can be expressed ubiquitously in various cell types, but in the present study, pMCAO induced strong expression of PAR-1 and PAR-2 in vascular cells (including PDGFRβ-positive cells) in ischemic areas, but much lower expression in neurons and astrocytes (Fig. 3A). PDGFRβ is a marker of pericytes and is highly upregulated in pericytes that participate in mature angiogenesis and subsequent fibrotic responses within ischemic areas. Thus, the co-expression of PDGFRβ and PAR1/PAR-2 in vascular cells within ischemic areas *in vivo,* combined with the finding that PAR1 and/or PAR2 inhibitors attenuated the survival/growth of cultured pericytes, suggest that factor Xa plays an important role in the survival/growth of pericytes, leading to the subsequent responses within ischemic areas after pMCAO (Ossovskaya and Bunnett, 2004; Vergnolle et al., 2001). Indeed, it is reported that PAR-2 signaling is sufficient for a pro-angiogenic effect under ischemic conditions (Uusitalo-Jarvinen et al., 2007). Moreover, Jin et al. demonstrated that infarct volume is increased and peri-infarct astrogliosis is reduced in PAR-2-deficient mice, although their focus was mainly on PAR-2 expression in neurons and glial cells within 24 h of tMCAO (Jin et al., 2005).

3.3. Factor Xa inhibition can affect intra-infarct angiogenesis, fibrotic responses, and inflammation in brain ischemia

PDGFRβ-positive pericytes and their derivatives (fibroblast-like cells) mediate intra-infarct angiogenesis and subsequent fibrotic responses in brain infarcts (Goritz et al., 2011; Makihara et al., 2015). Fibrosis is generally considered to be detrimental in chronic disease states because it may hinder tissue regeneration (Dias et al., 2018; Mack, 2018). However, pericyte-derived PDGFRβ-positive fibroblast-like cells can produce various neurotrophic factors and anti-

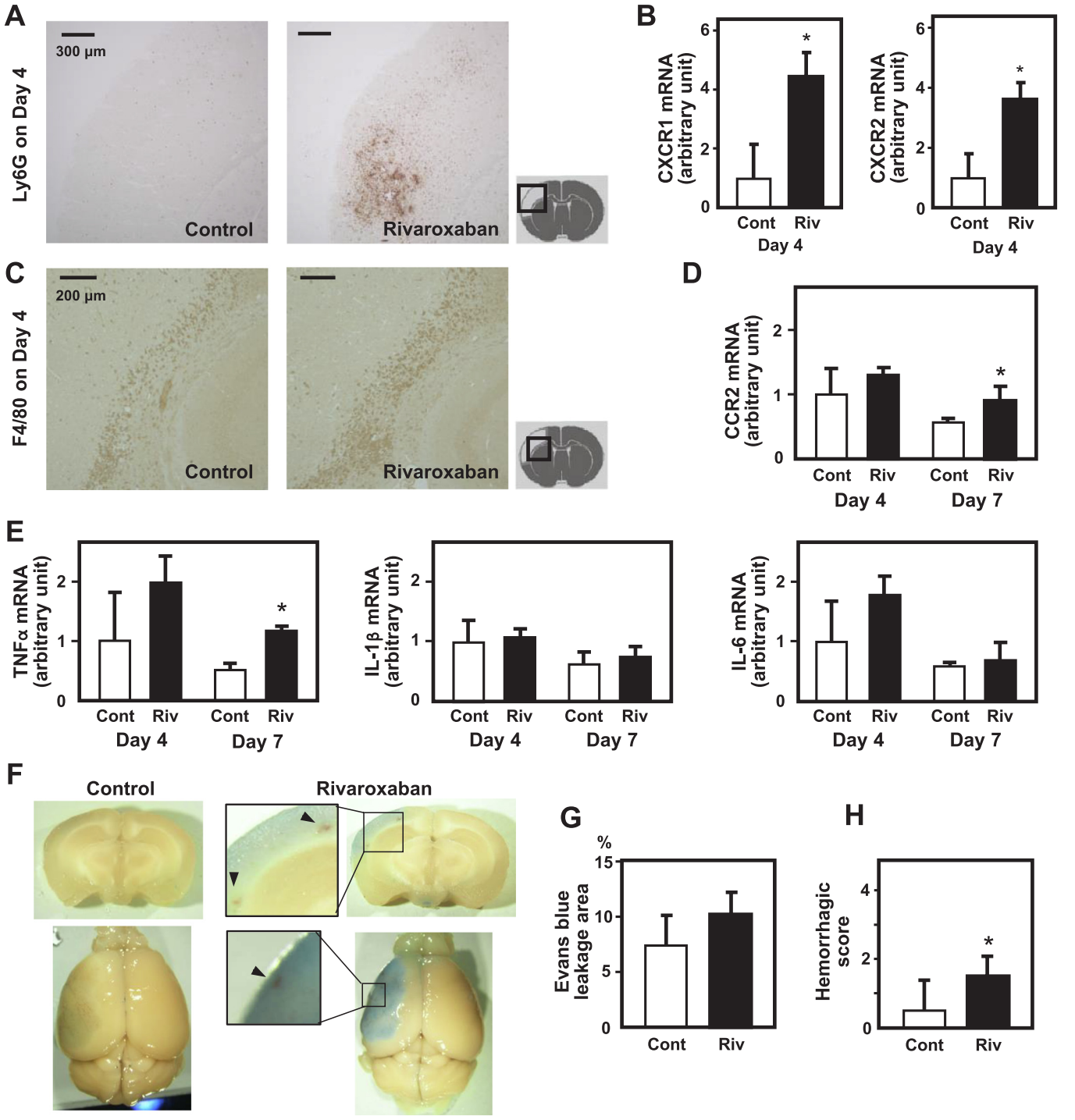

Fig. 4. Effects of rivaroxaban initiation immediately after pMCAO on inflammatory responses in ischemic areas. (A) Immunohistochemistry for Ly6G on day 4 after pMCAO in control and rivaroxaban-fed mice ($n = 4$). (B) Quantification of mRNA expression of CXCR1 and CXCR2, markers of neutrophils, in the ischemic hemisphere on day 4 after pMCAO in control and rivaroxaban-fed mice ($n = 3$; $^*p < 0.05$). (C) Immunohistochemistry for F4/80 on day 4 after pMCAO in control and rivaroxaban-fed mice ($n = 4$). (D) Quantification of CCR2 mRNA expression, a marker of monocyte/macrophage, in the ischemic hemisphere on days 4 and 7 after pMCAO in control and rivaroxaban-fed mice ($n = 3$; $^*p < 0.05$). (E) Quantification of mRNA expression of proinflammatory molecules TNF-α (left), IL-1β (middle), and IL-6 (right) in the ischemic hemisphere on days 4 and 7 after pMCAO. Values are means ± S.D. ($n = 3$; $^*p < 0.05$). Representative images of the blood–brain barrier breakdown, assessed by Evans blue dye, on day 4 after pMCAO (F), and quantification of the leakage (G). Values are means ± S.D ($n = 6$). (H) Hemorrhagic scores in control and rivaroxaban-fed mice. Values are means ± S.D ($n = 6$; $^*p < 0.05$).

inflammatory molecules, promptly halting injury-associated inflammatory responses and thereby enhancing neuroprotection and neuronal reorganization in peri-infarct areas (Arimura et al., 2012; Caplan and Correa, 2011; Chen et al., 2014; Ishitsuka et al., 2012; Mack, 2018). Thus, we speculate that the attenuated pericyte survival/growth and subsequent fibrotic responses by factor Xa inhibitors may be accompanied by enhanced inflammatory responses within infarct areas.

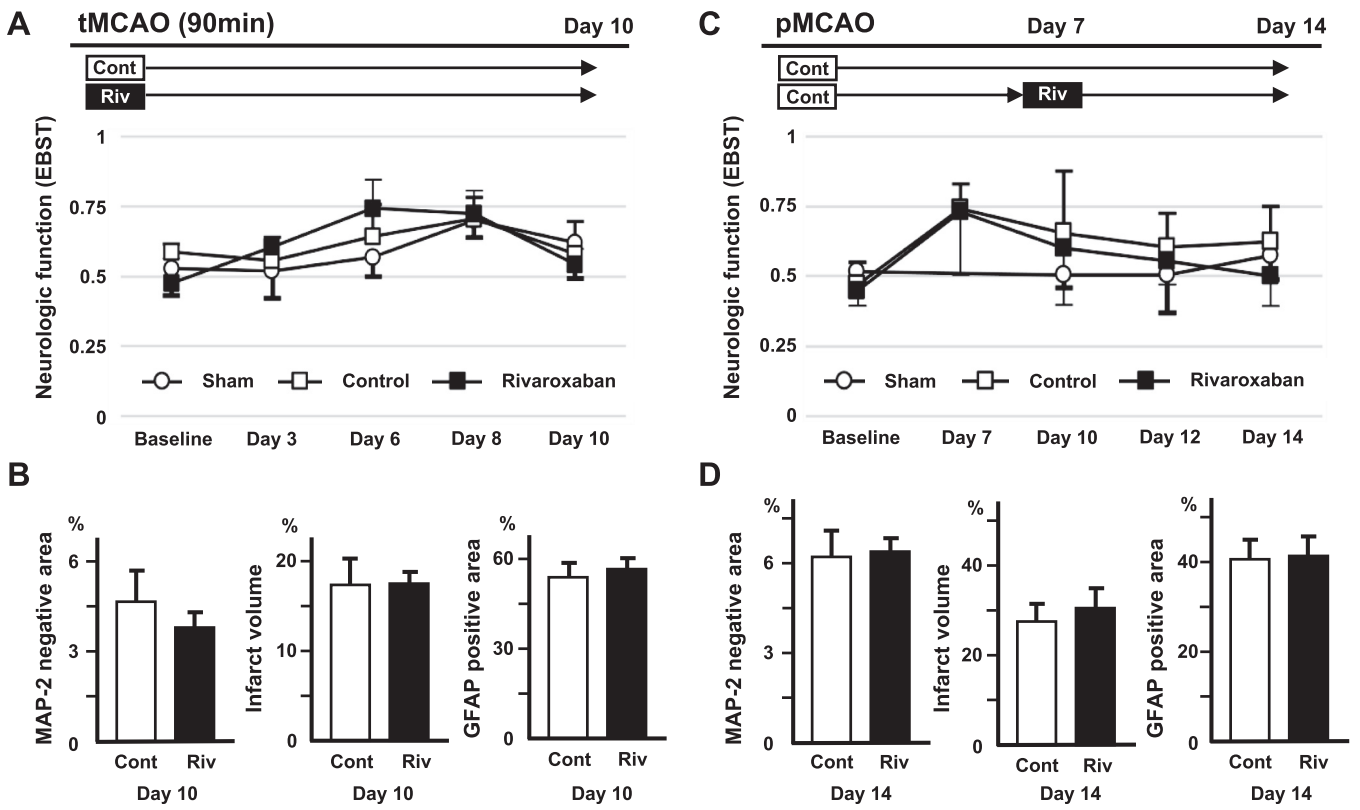

Fig. 5. Effects of rivaroxaban initiation immediately after tMCAO or of its delayed initiation after pMCAO on functional restoration or pathological changes. (A) Neurologic function assessed by EBST on days 3, 6, 8, and 10 after tMCAO (90 min ischemia and reperfusion) is shown in sham (non-pMCAO; open circle), control (open square), and rivaroxaban-fed (closed square) mice (n = 4). (B) MAP-2-negative areas (left), infarct volume (middle) and GFAP-positive areas (right) on day 10 after transient MCAO in control and rivaroxaban-fed mice (n = 4). (C) Neurologic function assessed by EBST on days 7, 10, 12, and 14 after pMCAO where rivaroxaban treatment was initiated on day 7 (n = 4). Sham (open circle), control (open square), and rivaroxaban-fed (closed square) mice (n = 4). (D) MAP-2-negative areas (left), infarct volume (middle) and GFAP-positive areas (right) on day 14 after pMCAO in control and rivaroxaban-fed mice (n = 5).

3.4. What is the difference between tMCAO and pMCAO in the use of factor Xa inhibitors?

It is reported that, in contrast to warfarin, pre-treatment with rivaroxaban before tMCAO with rt-PA infusion neither increases hemorrhages nor worsens neurologic functions in mice (Morihara et al., 2017; Ploen et al., 2014). Consistent with these reports, we demonstrated that rivaroxaban treatment initiated immediately after tMCAO affected neither histological changes nor neurologic function. We have recently reported that pericytes and endothelial cells are often intact within infarct areas after tMCAO, but not pMCAO: pericytes can survive and retain coverage of endothelial cells within infarct areas after tMCAO with short periods of ischemia (Tachibana et al., 2017). Therefore, angiogenic responses may not always be necessary after experimental tMCAO models, and unnecessary angiogenic responses may rather worsen BBB disruption and/or hemorrhage after tMCAO in the acute phase (Matsuo et al., 2013; Su et al., 2008; Zhang et al., 2000). However, because pericytes can easily die or detach from endothelial cells in the ischemic core after pMCAO, the angiogenic signaling related to pericyte survival/growth should be beneficial after pMCAO. Furthermore, because efficient reperfusion mediated by arteriogenesis and angiogenesis within infarct areas is usually achieved around day 7 after pMCAO, we may be able to safely initiate rivaroxaban treatment later than day 7 after pMCAO, even in the case of larger infarcts.

3.5. Clinical implications: the ideal timing for initiating anticoagulation therapy, including factor Xa inhibitors, in acute cardioembolic stroke

The timing of anti-coagulation therapy initiation remains controversial for patients with cardioembolic stroke in the acute phase. The present study suggests that we may be able to safely initiate anti-coagulation therapy, including with factor Xa inhibitors, by accurately judging the extent of effective reperfusion within ischemic areas, induced either by sufficient leptomeningeal anastomosis development or by successful recanalization of occluded large arteries. The present study may also support the clinically proposed “1-3-6-12 rule” (Heidbuchel et al., 2013) concept on the basis of arteriogenesis/angiogenesis, reperfusion, tissue repair, and functional restoration.

3.6. Limitations

In this study, we used CB-17 mice harboring few leptomeningeal anastomoses under healthy conditions (Tachibana et al., 2017; Zhang et al., 2010). Thus, the post-stroke recovery of blood flow and tissue repair within ischemic areas may be different in mice with different genetic backgrounds and leptomeningeal anastomoses at baseline (Zhang et al., 2010). In addition, we occluded the distal MCA completely by electrocauterization, to avoid spontaneous recanalization and to precisely examine leptomeningeal anastomosis development potential. It is important to note that early use of anti-coagulation therapy may induce spontaneous and unexpected recanalization of occluded arteries, thereby leading to different clinical courses, with better recovery of blood flow in some cases and with more massive hemorrhagic transformation in others.

In humans, rivaroxaban is administered once daily, causing peaks and troughs in its plasma concentration. However, in this study, rivaroxaban in a pellet chow was fed ad libitum to mice. We cannot exclude the possibility that a different administration schedule may affect factor Xa-mediated arteriogenesis/angiogenesis and subsequent tissue repair. However, we must note that the effects of rivaroxaban are

Table 1
The number of mice used in each experiment and related information.

Experiment	Model	Assignment	sacrifice schedule	numbers analyzed/ used	Body weight (g)	age (weeks)
Immunohistochemistry	pMCAO Rivaroxaban adm. on day 1	Control	day 4	4/5*	26.3 ± 3.8	10.9 ± 2.0
		Rivaroxaban		4/4	26.6 ± 3.4	11.8 ± 2.0
		Control	day 7	4/4	25.4 ± 1.8	9.2 ± 0.5
		Rivaroxaban		4/4	22.9 ± 1.4	8.4 ± 0.0
		Control	day 10	4/4	28.6 ± 0.4	11.5 ± 0.6
		Rivaroxaban		4/4	27.7 ± 0.9	11.5 ± 0.6
	pMCAO Rivaroxaban adm. on day 7	Control	day 14	5/5	27.4 ± 3.1	11.1 ± 1.9
		Rivaroxaban		5/5	26.2 ± 0.6	11.7 ± 1.7
	tMCAO Rivaroxaban adm. on day 1	Control	day 10	4/5*	29.3 ± 2.7	12.5 ± 2.0
		Rivaroxaban		4/5*	29.1 ± 0.9	11.6 ± 1.4
	Fixed frozen sample	Control	day 7	1/1	27.0	12.1
	subtotal			43/46		
EBST	pMCAO Rivaroxaban adm. on day 1	Sham	day 15	5/5	28.0 ± 1.7	13.0 ± 0.0
		Control		5/5	25.7 ± 3.4	10.9 ± 1.2
		Rivaroxaban		5/5	25.9 ± 1.6	11.3 ± 1.3
	pMCAO Rivaroxaban adm. on day 7	Control	day 15	4/4	32.1 ± 0.8	12.8 ± 0.3
		Rivaroxaban		4/4	30.9 ± 0.8	13.0 ± 0.4
	tMCAO Rivaroxaban adm. on day 1	Sham	day 10	4/4	27.6 ± 1.3	12.6 ± 0.8
		Control		4/4	28.7 ± 0.7	12.6 ± 1.4
		Rivaroxaban		4/4	29.9 ± 2.2	13.6 ± 1.5
	subtotal			35/35		
Visualization of brain angioarchitecture	day 1	Control	day 1	3/3	29.3 ± 0.3	13.2 ± 0.7
	day 4	Control	day 4	3/3	27.8 ± 1.3	11.5 ± 0.7
	pMCAO Rivaroxaban adm. on day 1	Control	day 7	4/6**	28.2 ± 0.4	12.1 ± 0.3
		Rivaroxaban		4/7**	28.5 ± 2.5	12.6 ± 1.4
	subtotal			14/19		
Werstern samples	day 10	Control	day 10	5/6*	26.5 ± 2.0	11.1 ± 1.5
		Rivaroxaban		5/5	27.5 ± 2.5	11.3 ± 1.1
	subtotal			10/11		
mRNA sample	pMCAO Rivaroxaban adm. on day 1	Control	day 4	3/3	29.3 ± 1.9	11.8 ± 0.8
		Rivaroxaban		3/3	27.4 ± 0.9	12.5 ± 0.1
		Control	day 7	3/3	26.0 ± 1.3	11.1 ± 1.5
		Rivaroxaban		3/4***	24.4 ± 1.7	10.0 ± 1.4
	subtotal			12/13		
Evans blue and quantification of hemorrhage	pMCAO Rivaroxaban adm. on day 1	Control	day 4	6/7***	28.3 ± 3.9	12.0 ± 2.1
		Rivaroxaban		6/6	26.9 ± 1.1	12.0 ± 0.3
	subtotal			12/13		
Exclude mice: MCA abnormality revealed during surgery				2		
	total			126/139		

Exclusion criteria: * Failure of surgery or incomplete reperfusion, ** Failure of latex perfusion, *** Premature death.

clearly different dependent upon tMCAO or pMCAO (Ploen et al., 2014); that is, they depend on the presence or absence of early recanalization that is highly associated with the vascular intactness of small vessels within the ischemic areas (Tachibana et al., 2017).

4. Experimental procedure

4.1. Animal stroke models

Animal experiments were conducted according to the Guidelines for Proper Conduct of Animal Experiments by the Science Council of Japan (Jun 1, 2006) (http://www.scj.go.jp/ja/info/kohyo/pdf/kohyo-20-k16-2e.pdf). The Animal Care and Use Review Committee of Kyushu University approved our animal procedures (Fukuoka, Japan) (A25-268-1). CB-17/lcr-+/+Jcl (CB-17) mice were purchased from CLEA Japan, Inc. (Tokyo, Japan). We used 139 male mice aged 8–16 weeks and weighing 21–36 g (Table 1), housed two per cage in the animal facility of Kyushu University at 21 °C and 65% humidity with a 12-hour light–dark cycle and free access to food and water. We gave CB-17 mice permanent or transient focal cerebral ischemia of the left MCA (pMCAO or tMCAO) using a modified Tamura's method as described previously (Tachibana et al., 2017). This stroke model is beneficial in both that infarct areas can be produced with high reproducibility and survival rates and that we can reduce the number of mice to be sacrificed (Taguchi et al., 2010). Mice were randomly assigned to the animal surgeon and were anesthetized by the inhalation of 2% isoflurane in air and maintained under anesthesia with 1.5% isoflurane. Rectal temperatures were maintained at 35–37 °C with a heating lamp. In the pMCAO model, the distal MCA was occluded by electrocauterization and completely disconnected to avoid spontaneous recanalization. In the tMCAO model, MCA occlusion was caused by rotating the suture 180° clockwise. During MCA occlusion, mice were kept in their cages without anesthesia until reperfusion. After 90 min of occlusion, mice were put under anesthesia and cerebral blood flow was restored by returning the nylon suture to its original position by counterclockwise rotation (Tachibana et al., 2017). Reduction and reperfusion of cerebral blood flow was confirmed using a 2D laser blood flow imager (OMEGAZONE OZ-2, OMEGAWAVE, INC., Japan) (Yukami et al., 2015). We initiated oral administration of rivaroxaban on day 1 or 7 after pMCAO, or on day 1 after tMCAO. Mice were fed ad libitum with a basic pellet chow containing 1200 ppm rivaroxaban, as reported previously (Morihara et al., 2017). We confirmed that prothrombin time-international normalized ratio (PT-INR), as measured with CoagCheck® XS Plus (Roche, Switzerland), was kept at around 1.6 in rivaroxaban-fed mice, while it was around 0.9 in control mice. The number of mice used in each experiment and related information is shown in Table 1. All experiments were reported according to the ARRIVE guidelines.

4.2. Assessment of neurologic function by EBST

Neurologic function was assessed by EBST with minor modifications in a blinded manner (Borlongan et al., 1995). Briefly, mice were held by the tail and elevated about 20 cm from the bottom of a transparent cage. During the 30 s trial, when mice moved more than 10° to the left or right of the vertical axis, the direction was recorded. In each trial, we scored the dominant side 1 point. If it was difficult to judge the dominant side, we scored 0.5 to each side. Each animal was returned to the vertical position before the next swing was started, and we repeated the trial 20 times. Although healthy mice do not exhibit a dominant side, mice after left MCAO swing dominantly to the contralateral (right) side. The final score was reported as the right-side score divided by 20.

4.3. Visualization of brain angioarchitecture by latex perfusion

Latex perfusion was performed as previously reported (Todo et al., 2008). Briefly, under deep pentobarbital anesthesia, the right atrium of the heart was incised to allow for venous outflow, the left ventricle of the heart was cannulated, and 5 ml saline was injected. Then, 0.5 ml of white latex compound (Product No. 563; Chicago Latex Products Inc.) mixed with 50 μL/mL carbon black was injected. Using stereoscopic microscope (Leica-MMI, Leica Microsystems), we counted the number of leptomeningeal anastomoses between the distal MCA and ACA or PCA, and measured their diameters at the confluent points.

4.4. Immunohistochemistry

Mice were sacrificed on the indicated day after MCAO by intraperitoneal administration of pentobarbital (150 mg/kg body weight) and injected with 20 ml ice-cold saline and 20 ml 4% paraformaldehyde (PFA) at 4 °C in phosphate-buffered saline (PBS) in the left atrium. Whole brains were fixed with 4% PFA in PBS for 3 days and cut into 2 mm slices. PFA-fixed coronal slices were embedded in paraffin and cut into 4 μm sections. For 3,3′-diaminobenzidine (DAB) staining, sections were deparaffinized, rehydrated through a graded ethanol series, and washed in PBS. Endogenous peroxidases were inactivated with 0.3% hydrogen peroxide for 30 min before blocking with 5% skim milk or PBS containing 10% normal goat serum for 30 min at room temperature. The sections were incubated with primary antibodies [mouse anti-MAP-2 (1:500–1:1000; Sigma-Aldrich, Tokyo, Japan), mouse anti-GFAP (1:100; Cell Signaling Technology, Boston, MA), rabbit anti-platelet-derived growth factor receptor β (PDGFRβ) (1:50–1:100; Cell Signaling Technology), rat anti-Ly6G (1:200; Abcam, Cambridge, UK), or rat anti-F4/80 (1:100; Abcam)] at 4 °C. After thorough washing, sections were incubated with appropriate secondary antibodies and stained with DAB using an appropriate kit (Nichirei, Tokyo, Japan). Sections were observed on a BIOREVO BZ-9000 microscope (Keyence Corporation, Osaka, Japan). For double labeling of MAP-2 and GFAP, sections were incubated overnight at 4 °C with MAP-2 antibody. The next day, after DAB staining of MAP-2, we performed epitope retrieval using microwave treatment for 25 min. After blocking with goat serum, sections were incubated with GFAP antibody at 4 °C overnight, and then visualized with Fast Red II (red) using a kit (Nichirei Bioscience Inc., Tokyo, Japan) (Tachibana et al., 2017). Measurement of immunopositive areas was performed using a total of three sections (approximately 0.6 mm anterior, and 1.4 mm and 3.4 mm posterior to the bregma) in a blinded manner (Tachibana et al., 2017). MAP2-negative areas (%) = (ipsilateral MAP2-negative area)/[(contralateral hemisphere)] × 100. Infarct volumes (%) = [(contralateral hemisphere) − (ipsilateral MAP2-positive areas)]/[(contralateral hemisphere)] × 100. GFAP-positive areas within MAP2-negative areas (%) = (ipsilateral GFAP-positive areas within MAP2-negative areas)/(MAP2-negative areas) × 100. For immunofluorescent double labelling with PDGFRβ or GFAP and PAR-1 or -2, frozen brains were serially sectioned in the coronal plane at 4 μm. Cryosections were washed with PBS, blocked with 5% skim milk for 30 min at room temperature, and incubated overnight at 4 °C with primary antibodies [goat anti-PDGFRβ (1:100; R & D systems, Minneapolis, MN), mouse anti-PAR-1 (1:100; Novus Biologicals, Centennial, CO) or mouse anti-PAR-2 (1:100; Santa Cruz Biotechnology, Dallas, TX)], followed by a 30-minute incubation with Alexa 488-conjugated chicken anti-mouse IgG (1:250) or goat anti-mouse IgG (1:250) and Alexa 568-conjugated goat anti-mouse (1:250) or donkey anti-goat IgG (1:250) (Thermo Fisher Scientific K.K., Japan), at room temperature. Samples were mounted with VECTASHIELD Mounting Medium (VECTOR Laboratories, CA, USA), and images were taken using the BIOREVO BZ-9000.

4.5. Quantification of BBB breakdown and intracerebral hemorrhage

Permeability of the BBB in the ischemic area was assessed by the leakage of Evans blue dye (Sigma-Aldrich). Brains were collected 180 min after a 2% solution of Evans blue dye (10 ml/kg body weight) was injected intraperitoneally (Manaenko et al., 2011). After injection of pentobarbital, mice were transcardially perfused with ice-cold saline and brains were cut into 2 mm thick coronal sections. Volumes of dye extravasation were determined by ImageJ: after the section color was split into 3-color channels, we measured the area of dye extravasation by subtracting the red channel from the blue channel in each section (x2-mm thick (mm^3)) and divided all the section volumes by the contralateral hemisphere (Tachibana et al., 2017). Quantification of the intracerebral hemorrhage on coronal sections and the brain surface was performed. Hemorrhagic scores were graded from 0 to 4: 0 = no hemorrhage, 1 = single petechial hemorrhage, 2 = confluent petechial hemorrhage, 3 = single space-occupying parenchymal hemorrhage encompassing < 30% of the infarction area, and 4 = multiple space-occupying parenchymal hemorrhages or a single space-occupying parenchymal hemorrhage encompassing > 30% of the infarction area (Ploen et al., 2014).

4.6. Cell culture

We used cultured human brain microvascular pericytes purchased from ScienCell Research Laboratories (CA, USA). The cells were plated on poly-L-lysine-coated dishes (Iwaki Glass, Japan) and cultured with the pericyte medium kit (ScienCell Research Laboratories) supplemented with 10% fetal bovine serum at 37 °C in 5% CO_2 in a humidified incubator.

4.7. MTS and LDH assay

Cultured pericytes were seeded onto 96-well plates at 5×10^3 cells/well. We treated the cells with factor Xa (50 nmol/L) for 96 h. Cell number was determined using the CellTiter96 Aqueous One Solution Cell Proliferation Assay kit (Promega), while cell toxicity (death) was determined using Cytotoxicity Detection Kit^{PLUS} (LDH) (Roche), with absorbance at 490 nm. When indicated, vorapaxar (5 μmol/L), an inhibitor of PAR-1, GB83 (10 μmol/L), an inhibitor of PAR-2, or rivaroxaban (10 μmol/L) was added to medium 1 h before the cells were treated with factor Xa.

4.8. Quantitative PCR

Total RNA was prepared from brain tissues or cultured pericytes using TRIzol (Thermo Fisher Scientific K.K.), and 1 μg of total RNA was reverse transcribed with a ReverTra Ace qPCR RT kit (Toyobo, Osaka, Japan). Using the reverse transcription product as a template, PCR was performed for 35 cycles with primers specific for the target genes. Quantitative PCR was performed in duplicate using a LightCycler (Roche, Mannheim, Germany) (Ishitsuka et al., 2012). The mRNA copy numbers were standardized using 18 s ribosomal RNA (rRNA) as an internal control (Makihara et al., 2015). Primers used in the present

study were: PAR-1 (human) (forward, 5′-CATTTGCTTCGGACCCA CAA-3′; reverse, 5′-TGCTGGGATCGGAACTTTCT-3′); PAR-2 (human) (forward, 5′-TTCCTCTCTCTGGCCATTGG-3′; reverse, 5′-GTCGATGCA GCTGTTAAGGG-3′); CXCR1 (mouse) (forward, 5′-TCAGTGGTATCCTG CTGCTG-3′; reverse, 5′-CTGGCGGAAGATAGCAAAAG-3′); CXCR2 (mouse) (forward, 5′-ATCTTCGCTGTCGTCCTTGT-3′; reverse, 5′-AGCC AAGAATCTCCGTAGCA-3′); CCR2 (mouse) (forward, 5′-ATTCTCCACA CCCTGTTTCG-3′; reverse, 5′-CTGCATGGCCTGGTCTAAGT-3′); TNF-α (mouse) (forward, 5′-CGTCAGCCGATTTGCTATCT-3′; reverse, 5′-CGG ACTCCGCAAAGTCTAAG-3′); IL-1β (mouse) (forward, 5′- GACTCATG GGATGATGATGATAAC -3′; reverse, 5′- CTCATGGAGAATATCACTTGT TGGT −3′); IL-6 (mouse) (forward, 5′-AGTTGCTTCTTGGGACTGA-3′; reverse, 5′-TCCACGATTTCCCAGAGAAC-3′); and 18s RNA (mouse) (forward, 5′-AAACGGCTACCACATCCAAG-3′; reverse, 5′-CCTCCAATG GATCCTCGTTA-3′).

4.9. Immunoblot analysis

Using brain homogenates prepared from the ischemic hemisphere after pMCAO, immunoblot analysis was performed as described previously (Tachibana et al., 2017). Equal amounts of proteins were subjected to SDS-PAGE and transferred onto PVDF membranes. The membranes were incubated for 1 h with ECL Advance blocking reagent (GE Healthcare, UK) at room temperature, and probed overnight at 4 °C with primary antibodies [GFAP (1:500; Cell Signaling Technology), PDGFRβ (1:500; Cell Signaling Technology), or β-actin (1:3000; Sigma-Aldrich)]. Membranes were then washed and incubated with secondary antibodies (1:100,000; Cell Signaling Technology) for 30 min at room temperature. Blots were developed using the ECL Advance Western Blotting Detection Kit (GE Healthcare). Quantification was performed densitometrically by ImageJ.

4.10. Statistical analysis

Statistical analyses were performed with JMP software (Version 12, SAS Institute, Cary, NC). All data are expressed as mean ± SD. Analyses between groups were performed with unpaired Student's *t*-test or ANOVA followed by a Bonferroni *post hoc* test. A two-way factorial ANOVA was used to compare functional restoration among groups. A value of $p < 0.05$ was regarded as statistically significant.

Sources of funding

The work was supported in part by a Grant-in-Aid for Scientific Research (B) (16H05439) (T.K. and T.A.) and (C) (26462163) (Y.W.) from the Ministry of Education, Culture, Sports, Science and Technology, Japan.

Disclosures

This work was partially supported by a research fund from Bayer Yakuhin, Ltd. The funders had no role in the study design, data collection, data analysis, or preparation of the manuscript.

Acknowledgments

We thank Naoko Kasahara (Hisayama Research Institute for Lifestyle Diseases) and Hideko Noguchi (Kyushu University) for technical support, and Maya Kanazawa (Kyushu University) for secretarial assistance. We thank Bronwen Gardner, PhD, from Edanz Group (www.edanzediting.com/ac) for editing a draft of this manuscript.

References

Arimura, K., Ago, T., Kamouchi, M., Nakamura, K., Ishitsuka, K., Kuroda, J., Sugimori, H., Ooboshi, H., Sasaki, T., Kitazono, T., 2012. PDGF receptor beta signaling in pericytes following ischemic brain injury. Curr. Neurovasc. Res. 9, 1–9.

Battinelli, E.M., Markens, B.A., Kulenthirarajan, R.A., Machlus, K.R., Flaumenhaft, R., Italiano Jr., J.E., 2014. Anticoagulation inhibits tumor cell-mediated release of platelet angiogenic proteins and diminishes platelet angiogenic response. Blood 123, 101–112.

Berger, C., Fiorelli, M., Steiner, T., Schabitz, W.R., Bozzao, L., Bluhmki, E., Hacke, W., von Kummer, R., 2001. Hemorrhagic transformation of ischemic brain tissue: asymptomatic or symptomatic? Stroke 32, 1330–1335.

Bodnar, R.J., Rodgers, M.E., Chen, W.C., Wells, A., 2013. Pericyte regulation of vascular remodeling through the CXC receptor 3. Arterioscler. Thromb. Vasc. Biol. 33, 2818–2829.

Borlongan, C.V., Cahill, D.W., Sanberg, P.R., 1995. Locomotor and passive-avoidance deficits following occlusion of the middle cerebral-artery. Physiol. Behav. 58, 909–917.

Caplan, A.I., Correa, D., 2011. The MSC: an injury drugstore. Cell Stem Cell 9, 11–15.

Chen, J., Venkat, P., Zacharek, A., Chopp, M., 2014. Neurorestorative therapy for stroke. Front. Hum. Neurosci. 8, 382.

Dias, D.O., Kim, H., Holl, D., Werne Solnestam, B., Lundeberg, J., Carlen, M., Goritz, C., Frisen, J., 2018. Reducing pericyte-derived scarring promotes recovery after spinal cord injury. Cell 173 (153–165), e122.

Gage, B.F., Waterman, A.D., Shannon, W., Boechler, M., Rich, M.W., Radford, M.J., 2001. Validation of clinical classification schemes for predicting stroke: results from the National Registry of Atrial Fibrillation. JAMA 285, 2864–2870.

Gioia, L.C., Kate, M., Sivakumar, L., Hussain, D., Kalashyan, H., Buck, B., Bussiere, M., Jeerakathil, T., Shuaib, A., Emery, D., Butcher, K., 2016. Early rivaroxaban use after cardioembolic stroke may not result in hemorrhagic transformation: a prospective magnetic resonance imaging study. Stroke 47, 1917–1919.

Goritz, C., Dias, D.O., Tomilin, N., Barbacid, M., Shupliakov, O., Frisen, J., 2011. A pericyte origin of spinal cord scar tissue. Science 333, 238–242.

Heidbuchel, H., Verhamme, P., Alings, M., Antz, M., Hacke, W., Oldgren, J., Sinnaeve, P., Camm, A.J., Kirchhof, P., European Heart Rhythm, A., 2013. European Heart Rhythm Association Practical Guide on the use of new oral anticoagulants in patients with non-valvular atrial fibrillation. Europace 15, 625–651.

Ishitsuka, K., Ago, T., Arimura, K., Nakamura, K., Tokami, H., Makihara, N., Kuroda, J., Kamouchi, M., Kitazono, T., 2012. Neurotrophin production in brain pericytes during hypoxia: a role of pericytes for neuroprotection. Microvasc. Res. 83, 352–359.

Jin, G., Hayashi, T., Kawagoe, J., Takizawa, T., Nagata, T., Nagano, I., Syoji, M., Abe, K., 2005. Deficiency of PAR-2 gene increases acute focal ischemic brain injury. J. Cereb. Blood Flow Metab. 25, 302–313.

Katsanos, K., Karnabatidis, D., Diamantopoulos, A., Kagadis, G.C., Ravazoula, P., Nikiforidis, G.C., Siablis, D., Tsopanoglou, N.E., 2009. Thrombin promotes arteriogenesis and hemodynamic recovery in a rabbit hindlimb ischemia model. J. Vasc. Surg. 49, 1000–1012.

Kernan, W.N., Ovbiagele, B., Black, H.R., Bravata, D.M., Chimowitz, M.I., Ezekowitz, M.D., Fang, M.C., Fisher, M., Furie, K.L., Heck, D.V., Johnston, S.C., Kasner, S.E., Kittner, S.J., Mitchell, P.H., Rich, M.W., Richardson, D., Schwamm, L.H., Wilson, J.A., American Heart Association Stroke Council CoC, 2014. Guidelines for the prevention of stroke in patients with stroke and transient ischemic attack: a guideline for healthcare professionals from the American Heart Association/American Stroke Association. Stroke 45, 2160–2236.

Mack, M., 2018. Inflammation and fibrosis. Matrix Biol. 68–69, 106–121.

Makihara, N., Arimura, K., Ago, T., Tachibana, M., Nishimura, A., Nakamura, K., Matsuo, R., Wakisaka, Y., Kuroda, J., Sugimori, H., Kamouchi, M., Kitazono, T., 2015. Involvement of platelet-derived growth factor receptor beta in fibrosis through extracellular matrix protein production after ischemic stroke. Exp. Neurol. 264, 127–134.

Manaenko, A., Chen, H., Kammer, J., Zhang, J.H., Tang, J., 2011. Comparison Evans Blue injection routes: Intravenous versus intraperitoneal, for measurement of blood-brain barrier in a mice hemorrhage model. J. Neurosci. Methods 195, 206–210.

Matsuo, R., Ago, T., Kamouchi, M., Kuroda, J., Kuwashiro, T., Hata, J., Sugimori, H., Fukuda, K., Gotoh, S., Makihara, N., Fukuhara, M., Awano, H., Isomura, T., Suzuki, K., Yasaka, M., Okada, Y., Kiyohara, Y., Kitazono, T., 2013. Clinical significance of plasma VEGF value in ischemic stroke - research for biomarkers in ischemic stroke (REBIOS) study. BMC Neurol. 13, 32.

Mercer, P.F., Chambers, R.C., 2013. Coagulation and coagulation signalling in fibrosis. Biochim. Biophys. Acta 1832, 1018–1027.

Morihara, R., Yamashita, T., Kono, S., Shang, J., Nakano, Y., Sato, K., Hishikawa, N., Ohta, Y., Heitmeier, S., Perzborn, E., Abe, K., 2017. Reduction of intracerebral hemorrhage by rivaroxaban after tPA thrombolysis is associated with downregulation of PAR-1 and PAR-2. J. Neurosci. Res. 95, 1818–1828.

Ossovskaya, V.S., Bunnett, N.W., 2004. Protease-activated receptors: contribution to physiology and disease. Physiol. Rev. 84, 579–621.

Ploen, R., Sun, L., Zhou, W., Heitmeier, S., Zorn, M., Jenetzky, E., Veltkamp, R., 2014. Rivaroxaban does not increase hemorrhage after thrombolysis in experimental ischemic stroke. J. Cereb. Blood Flow Metab. 34, 495–501.

Renner, O., Tsimpas, A., Kostin, S., Valable, S., Petit, E., Schaper, W., Marti, H.H., 2003. Time- and cell type-specific induction of platelet-derived growth factor receptor-beta during cerebral ischemia. Brain Res. Mol. Brain Res. 113, 44–51.

Shichita, T., Ago, T., Kamouchi, M., Kitazono, T., Yoshimura, A., Ooboshi, H., 2012. Novel therapeutic strategies targeting innate immune responses and early inflammation after stroke. J. Neurochem. 123 (Suppl 2), 29–38.

Striggow, F., Riek, M., Breder, J., Henrich-Noack, P., Reymann, K.G., Reiser, G., 2000. The protease thrombin is an endogenous mediator of hippocampal neuroprotection against ischemia at low concentrations but causes degeneration at high concentrations. Proc. Natl. Acad. Sci. U.S.A. 97, 2264–2269.

Su, E.J., Fredriksson, L., Geyer, M., Folestad, E., Cale, J., Andrae, J., Gao, Y., Pietras, K.,

Mann, K., Yepes, M., Strickland, D.K., Betsholtz, C., Eriksson, U., Lawrence, D.A., 2008. Activation of PDGF-CC by tissue plasminogen activator impairs blood-brain barrier integrity during ischemic stroke. Nat. Med. 14, 731–737.
Tachibana, M., Ago, T., Wakisaka, Y., Kuroda, J., Shijo, M., Yoshikawa, Y., Komori, M., Nishimura, A., Makihara, N., Nakamura, K., Kitazono, T., 2017. Early reperfusion after brain ischemia has beneficial effects beyond rescuing neurons. Stroke 48, 2222–2230.
Taguchi, A., Kasahara, Y., Nakagomi, T., Stern, D.M., Fukunaga, M., Ishikawa, M., Matsuyama, T., 2010. A reproducible and simple model of permanent cerebral ischemia in CB-17 and SCID mice. J. Exp. Stroke Transl. Med. 3, 28–33.
Todo, K., Kitagawa, K., Sasaki, T., Omura-Matsuoka, E., Terasaki, Y., Oyama, N., Yagita, Y., Hori, M., 2008. Granulocyte-macrophage colony-stimulating factor enhances leptomeningeal collateral growth induced by common carotid artery occlusion. Stroke 39, 1875–1882.
Uusitalo-Jarvinen, H., Kurokawa, T., Mueller, B.M., Andrade-Gordon, P., Friedlander, M., Ruf, W., 2007. Role of protease activated receptor 1 and 2 signaling in hypoxia-induced angiogenesis. Arterioscler. Thromb. Vasc. Biol. 27, 1456–1462.
Vergnolle, N., Wallace, J.L., Bunnett, N.W., Hollenberg, M.D., 2001. Protease-activated receptors in inflammation, neuronal signaling and pain. Trends Pharmacol. Sci. 22, 146–152.
Yukami, T., Yagita, Y., Sugiyama, Y., Oyama, N., Watanabe, A., Sasaki, T., Sakaguchi, M., Mochizuki, H., Kitagawa, K., 2015. Chronic elevation of tumor necrosis factor-alpha mediates the impairment of leptomeningeal arteriogenesis in db/db Mice. Stroke 46, 1657–1663.
Zhang, H., Prabhakar, P., Sealock, R., Faber, J.E., 2010. Wide genetic variation in the native pial collateral circulation is a major determinant of variation in severity of stroke. J. Cereb. Blood Flow Metab. 30, 923–934.
Zhang, Z., Zhang, L., Jiang, Q., Zhang, R., Davies, K., Powers, C., Bruggen, N., Chopp, M., 2000. VEGF enhances angiogenesis and promotes blood–brain barrier leakage in the ischemic brain. J. Clin. Invest. 106, 829–838.